Cancer Science
Japanese Cancer Association JCA
Open Access

Silencing of STRN4 suppresses the malignant characteristics of cancer cells

Meihong Wong,[1] Toshinori Hyodo,[2] Eri Asano,[2] Kohei Funasaka,[1] Ryoji Miyahara,[1] Yoshiki Hirooka,[1] Hidemi Goto,[1] Michinari Hamaguchi[2] and Takeshi Senga[2]

[1]Department of Gastroenterology and Hepatology; [2]Division of Cancer Biology, Nagoya University Graduate School of Medicine, Nagoya, Japan

Key words
Anoikis, invasion, migration Striatin, STRN4, STRIPAK

Correspondence
Takeshi Senga, Division of Cancer Biology, Nagoya University Graduate School of Medicine, 65 Tsurumai-cho, Showa-ku, Nagoya 466-8550, Japan.
Tel: +81-52-744-2463; Fax: +81-52-744-2464;
E-mail: tsenga@med.nagoya-u.ac.jp

Funding Information
Naito Foundation and the Ministry of Education, Culture, Sports, Science and Technology of Japan

Received April 10, 2014; Revised August 17, 2014; Accepted September 18, 2014

Cancer Sci **105** (2014) 1526–1532

doi: 10.1111/cas.12541

The striatin family of proteins, comprising STRN, STRN3 and STRN4, are multidomain-containing proteins that associate with additional proteins to form a large protein complex. We previously reported that STRN4 directly associated with protein kinases, such as MINK1, TNIK and MAP4K4, which are associated with tumor suppression or tumor progression. However, it remains unclear whether STRN4 is associated with tumor progression. In this report, we examined the role that STRN4 plays in cancer malignancy. We show that depletion of STRN4 suppresses proliferation, migration, invasion and the anchorage-independent growth of cancer cells. In addition, STRN4 knockdown increases the sensitivity of pancreatic cancer cells to gemcitabine. Finally, we show that STRN4 knockdown suppresses the proliferation and metastasis of cancer cells in mice. Our results demonstrate a possible role of STRN4 in tumor progression.

STRN (striatin), STRN3 (SG2NA) and STRN4 (Zinedin) are members of the striatin family of proteins that contain multiple protein-binding domains, such as a caveolin-binding domain, a coiled-coil domain, a Ca^{2+}-calmodulin-binding domain and a WD-repeat domain.[1–3] These domains mediate the dimerization of striatin family members and the association with a diverse set of proteins, including calmodulin and caveolin.[4–6] The striatin family proteins are highly expressed in the central and peripheral nervous systems, and partial knockdown of striatin in the rat brain and rat neuron cultures induces a decrease in nocturnal locomotor activity and defects in dendritic growth, respectively.[7–9] The striatin family is also expressed in additional tissues and cell lines, and these proteins are reported to regulate the localization of the tight junction protein ZO1 and the estrogen-induced activation of endothelial NO synthase.[10,11]

Striatin family proteins are also known to form a complex with protein phosphatases and protein kinases.[12,13] Accumulating evidence has revealed that striatin family proteins act as a regulatory subunit of protein phosphatase 2A (PP2A).[14,15] PP2A is a heterotrimeric complex of catalytic, structural and regulatory subunits and regulates the signaling pathways involved in cell proliferation, differentiation, apoptosis and transformation.[16,17] Recent studies have revealed that PP2A holoenzymes containing striatins are core components of a large protein complex called striatin-interacting phosphatase and kinase (STRIPAK).[18,19] The STRIPAK complex is conserved in a wide range of species and is thought to play a crucial role in fundamental biological processes.[20–23] We have previously reported that a member of the striatin family, STRN4, is associated with members of the germinal center kinase family, including misshapen-like kinase 1 (MINK1), Traf2- and NCK-interacting protein (TNIK) and mitogen-activated protein kinase kinase kinase kinase 4 (MAP4K4).[13] Although the exact function of these kinases remains uncertain, several lines of evidence have revealed that they exert tumor promoting or tumor suppressing activity.[24–26] However, whether STRN4, an interacting partner of these kinases, is associated with tumor progression remains unknown. In this report, using multiple cancer cell lines, we examine the role that STRN4 plays in cancer progression.

Materials and Methods

Cells and antibodies. All cell lines were cultured in RPMI or DMEM with 10% FBS and antibiotics. The following cancer cell lines were used: KP4 and PK9 (pancreatic cancer), TE1 (esophageal cancer), MKN28 (gastric cancer), HCT116 (colorectal cancer), LU65 (lung cancer), BT20 (breast cancer) and SKOV3 (ovarian cancer). Anti-STRN4 antibody was generated using aa1-147 of STRN4 fused with GST.[13]

siRNA transfection. siRNA were obtained from Sigma-Aldrich (St. Louis, MO, USA). The sequences of siRNA used to knockdown STRN4 are as follows: 5′-GCUAUGUGAACC UAUATT-3′ (siSTRN4-1), 5′-UAUAGGUUCCACAUCUAG CTT-3′ (siSTRN4-2) and 5′-GCCUCUGUCUGUUUGCCAUT T-3′ (siSTRN4-3). The sequence of the control siRNA that targets luciferase is 5′-CUUACGCUGAGUACUUCGATT-3′. The cells were transfected with 50 nM of the siRNA using

Lipofectamine RNAiMAX (Invitrogen, Carlsbad, CA, USA) according to the manufacturer's instructions.

Generation of stable cell lines. To produce KP4 cells that constitutively expressed shRNA, oligonucleotides encoding shRNA specific for STRN4 (5′-GCTATGTGAACCTATA-3′) and luciferase (5′-CTTACGCTGAGTACTTCGA-3′) were cloned into the pSIREN-RetroQ retroviral vector (Clontech, Mountain View, CA, USA). Next, 293T cells were transfected with the pSIREN-RetroQ vector encoding each shRNA as well as the pVPack-GP and pVPack-Ampho vectors (Stratagene, Tokyo, Japan). The culture supernatant was collected 48 h later and applied to KP4 cells with 2 μg/mL of polybrene (Sigma-Aldrich). The cells were cultured for 24 h, and 1 μg /mL of puromycin (Sigma-Aldrich) was then added to the culture to select for infected cells. KP4 cells that constitutively expressed Flag tag or STRN4 were established by retroviral infection and selection with puromycin.

Proliferation assay. Cells were reverse transfected with siRNA using Lipofectamine RNAiMAX, and 1000 cells were seeded into each well of a 96-well plate. The next day of transfection was set as day 0, and the number of viable cells at the indicated time points were evaluated using Cell Count Kit-8 (Dojindo, Tokyo, Japan). To determine the cell proliferation ratio in the presence of gemcitabine, cells were cultured in 96-well plates with various concentrations of gemcitabine in triplicate. Three days later, the number of viable cells was evaluated using Cell Count Kit-8.

EdU incorporation assay. The thymidine nucleotide analog 5-ethynyl-2′-deoxyuridine (EdU) was used for the *in vitro* labeling of cell nuclei. Cells were transfected with siRNA, and 48 h later, EdU incorporation assays were performed using Click-iT Plus EdU Alexa Fluor 594 Imaging Kit (Life Technologies, Carlsbad, CA, USA). Briefly, half of the media was replaced with fresh media containing 20 μM EdU and incubated for another 24 h. Cells were fixed with formaldehyde, permeabilized with 0.5% Triton X-100 and stained with a reaction cocktail and Hoechst according to the manufacturer's instructions. Cells were imaged with fluorescence microscopy, and the percentage of EdU-positive cells was evaluated.

Invasion assay. To measure cell invasion using 24-well Boyden chambers (8-μm pore size, 6.5-mm membrane diameter), the filter was pre-coated with Matrigel (BD Biosciences, San Jose, CA, USA) and 1.5×10^5 cells were seeded onto the upper surface of the chamber. Sixteen hours after seeding, the cells were fixed with 100% ethanol and stained with 0.5% crystal violet. Cells that invaded the lower surface of the filters were surveyed under a microscope at 100× magnification, and five fields were randomly selected. Three independent experiments were performed.

Migration assay. Wound healing assays were performed by scratching confluent monolayers of siRNA-transfected cells with a 200-μL pipette tip and incubating the cells at 37°C with 5% CO_2. Twenty-four hours later, the distance between the leading edges of the monolayer was measured in five randomly selected fields. Three independent experiments were performed. To measure cell migration using 24-well Boyden chambers (8-μm pore size and 6.5-mm membrane diameter), 5×10^4 cells were seeded onto the upper surface of the chamber. The lower surface of the filter was coated with fibronectin. Six hours after seeding, the cells were fixed with 100% ethanol and stained with 0.5% crystal violet. Cells that migrated to the lower surface of the chambers were surveyed under a microscope at 100× magnification, and five fields were randomly selected. Three independent experiments were performed.

Anoikis assay. siRNA-transfected cells were mixed with 1.68% methyl cellulose in medium and incubated for 48 h. After incubation, the cells were collected via centrifugation and subjected to a TUNEL assay using the In Situ Cell Death Detection Kit (Roche, Basel, Switzerland) according to the manufacturer's protocol.

Colony formation assay. Cells (1×10^4) were mixed with 0.36% agar in RPMI or DMEM supplemented with 10% FBS and overlaid onto a 0.72% agarose layer in 6-well plates. After 2 weeks of incubation, colonies in five randomly selected fields were counted. Three independent experiments were performed.

Animal experiments. Animal experiments were conducted in accordance with the regulations of the Faculty of Mefdicine of Nagoya University. A total of 1×10^6 shCtrl and shSTRN4-1 KP4 cells were suspended in 0.1 mL PBS and injected s.c. into both sides of the femoral area of five nude mice. The tumors were measured with calipers, and tumor volume was calculated using the following formula: $\pi /6 \times (\text{largest diameter})^3$. Five weeks after tumor inoculation, the mice were killed and the tumors were extracted to determine tumor weight. To examine metastasis of the cancer cells, 2×10^6 cells in 200 μL PBS were injected into the lateral tail vein of mice using a 23G needle. Five mice were used for each cell line. Two months after the injections, the mice were killed and the metastatic foci in the lung and liver were examined. Metastatic tissues were fixed in paraffin and stained with HE. The surviving mice were killed 8 weeks after the injections.

Results

Suppression of STRN4 inhibits the proliferation of cancer cells. To examine whether STRN4 plays a functional role in cancer, we examined the expression of STRN4 in multiple cancer cell lines. Immunoblot analysis using an affinity-purified anti-STRN4 antibody revealed that STRN4 was expressed in multiple cancer cell lines (Fig. 1a). We then used siRNA to deplete STRN4 expression. Cells were transfected with two different STRN4 siRNA. After 72 h, the expression of STRN4 was examined. siRNA efficiently suppressed the expression of STRN4 in all the cell lines (Fig. S1). Using these siRNA, we investigated the proliferation of STRN4-depleted cells. Cells were transfected with siRNA, and the number of viable cells at the indicated time points was determined using Cell Counting Kit-8, which measures cellular dehydrogenase activity. Although proliferation of KP4, PK9 and HCT116 cells was clearly reduced by STRN4 knockdown, STRN4 depletion did not affect the growth of SKOV3 or LU65 cells (Fig. 1b). Minor reduction of proliferation by STRN4 knockdown was observed in TE1, MKN28 and BT20 cells (Fig. 1b). To determine whether the reduction in proliferation of KP4, PK9 and HCT116 cells was mediated by the inhibition of cell cycle progression or by the induction of apoptosis, we performed an EdU incorporation assay and a TUNEL assay. EdU is a thymidine analog and is incorporated into newly synthesized DNA during S phase. As shown in Figure 1(c), depletion of STRN4 significantly reduced the ratio of EdU-positive cells. The TUNEL assay demonstrated an induction of apoptosis by STRN4 depletion in KP4, PK9 and HCT116 cells (Figs 1d, S1b). These results indicate that the reduction of proliferation by STRN4 knockdown is mediated by both

the inhibition of cell cycle progression and the induction of apoptosis.

STRN4 knockdown inhibits cell migration and invasion. We next investigated whether STRN4 knockdown affects cell migration and invasion. To assess changes in cell migration, we first performed a wound healing assay. Confluent monolayers of KP4, HCT116, TE1 and SKOV3 cells transfected with siRNA were scratched, and the migration of the cells into the free space was observed 24 h later. The migration of STRN4-depleted cells was clearly delayed compared with that of the control siRNA-transfected cells (Fig. 2a). To further confirm this result, we used a modified Boyden chamber assay. Cells transfected with siRNA were placed on the upper surface of the filter and allowed to migrate to the bottom surface, which was coated with fibronectin. Cells that migrated to the bottom surface were quantified. The migration of STRN4-depleted cells was suppressed compared with that of the control siRNA-transfected cells (Figs 2b, S2a). To investigate the effect that STRN4 suppression had on cell invasion, we used a Matrigel-coated Boyden chamber. The invasion of cancer cells was significantly reduced by STRN4 knockdown (Figs 2c, S2b). To exclude the possibility that the suppression of cell migration and invasion was an off-target effect of siRNA, we performed a rescue experiment using KP4 cells. We first established KP4 cell lines that constitutively expressed a Flag tag (Flag-KP4) or STRN4 (STRN4-KP4) by retroviral infection. We then used siRNA that targeted the 3′ UTR of STRN4 (siSTRN4-3). Transfection of siSTRN4-3 efficiently suppressed the endogenous STRN4 in Flag-KP4 cells but not the exogenously expressed STRN4 in STRN4-KP4 cells (Fig. 2d). The expression of exogenous STRN4 clearly rescued the suppression of migration and the invasion induced by siSTRN4-3 transfection (Fig. 2e). These results indicate that STRN4 depletion suppresses cell migration and invasion.

STRN4 knockdown suppresses anchorage-independent growth and promotes anoikis. We next assessed the anchorage-independent growth of the STRN4-depleted cells. Among the cancer cell lines we tested, KP4, PK9, HCT116, TE1 and SKOV3 formed colonies when cultured in the soft agar; therefore, we used these cell lines for the colony formation assay. siRNA-transfected cells were cultured in soft agar, and colony formation was evaluated 2 weeks later. The STRN4 siRNA-transfected cells formed significantly fewer colonies than the control siRNA-transfected cells (Fig. 3a). To confirm that the

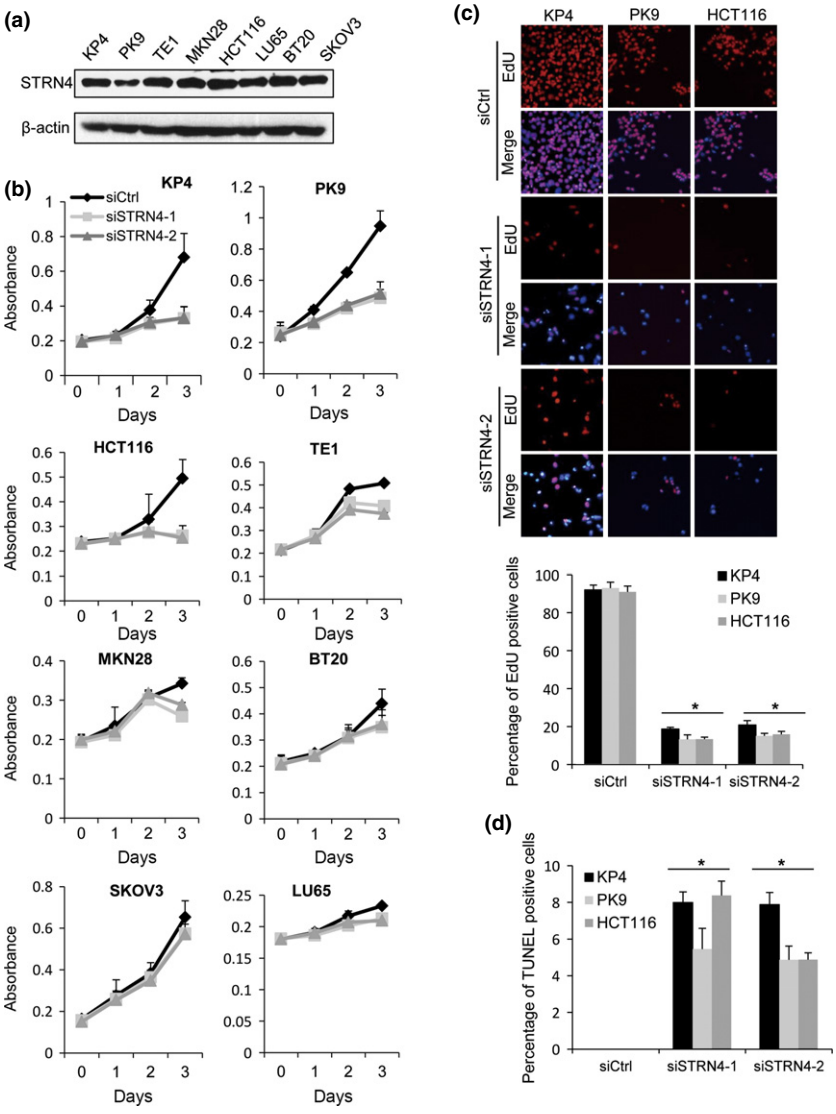

Fig. 1. STRN4 knockdown reduces the proliferation of cancer cells. (a) Expression of STRN4 was examined via immunoblot. (b) Cells were transfected with siRNA, and the number of viable cells at the indicated time points was evaluated. (c) Cells were transfected with siRNA, and 48 h later, the cells were subjected to EdU incorporation assay. Representative pictures are shown, and the graph indicates the percentage of EdU positive cells. Three independent experiments were performed, and the data are shown as the mean ± SD (*$P < 0.05$, compared with Ctrl siRNA-transfected cells). (d) Cells were transfected with siRNA, and 72 h later, the cells were subjected to TUNEL assay. The graph indicates the percentage of TUNEL positive cells. There were no TUNEL positive cells in the control siRNA-transfected cells; hence, there is no value for siCtrl. Three independent experiments were performed, and the data are shown as the mean ± SD (*$P < 0.05$, compared with Ctrl siRNA-transfected cells).

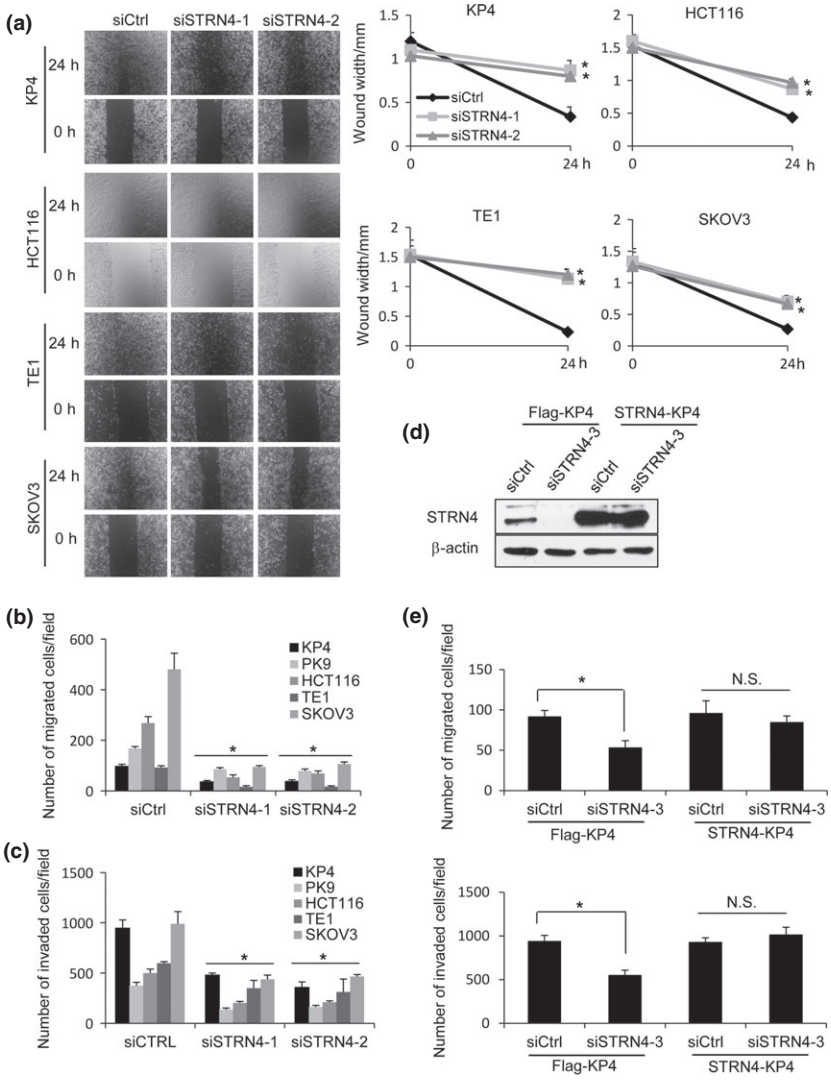

Fig. 2. Silencing of STRN4 inhibits cell migration and invasion. (a) Monolayers of siRNA-transfected cells were scratched, and the distance between the leading edges was measured 24 h later. Representative images of the cells are shown. The graph shows the average distance of wound healing. Three independent experiments were performed, and the data are shown as the mean ± SD (*$P < 0.05$, compared with Ctrl siRNA-transfected cells). (b) Cells were transfected with siRNA, and 72 h later, cell migration was examined. The graph indicates the average number of migrated cells per field. Three independent experiments were performed, and the data are shown as the mean ± SD (*$P < 0.05$, compared with Ctrl siRNA-transfected cells). (c) siRNA-transfected cells were subjected to invasion assay. The graph indicates the average number of invaded cells per field. Three independent experiments were performed, and the data are shown as the mean ± SD (*$P < 0.05$, compared with Ctrl siRNA-transfected cells). (d) KP4 cells that constitutively expressed Flag tag (Flag-KP4) or STRN4 (STRN4-KP4) were established by retroviral infection. Cells were transfected with siRNA, and 72 h later, expression of STRN4 was examined by immunoblot. (e) Cells were transfected with siRNA, and 72 h later, the cells were subjected to migration and invasion assay. The graph indicates the average number of migrated or invaded cells per field. Three independent experiments were performed, and the data are shown as the mean ± SD (*$P < 0.05$; NS, not significant).

suppression of colony formation was mediated by STRN4 depletion, we performed a rescue experiment. STRN4-expressing KP4 cells were transfected with siSTRN4-3 and subjected to colony formation. The exogenous expression of STRN4 clearly inhibited the suppression of colony formation by siSTRN4-3 transfection (Fig. 3b). Anoikis is a form of cell apoptosis induced by the detachment of cells from the extracellular matrix. We hypothesized that the suppression of colony formation by STRN4 knockdown was associated with the promotion of anoikis. Cells transfected with siRNA were cultured in suspension for 48 h, and apoptotic cells were then detected via TUNEL assay. As shown in Figure 3(c), STRN4 depletion clearly increased the ratio of apoptotic cells after 48 h of suspension culture. A rescue experiment confirmed that the induction of anoikis was mediated by STRN4 depletion (Fig. 3d).

STRN4 knockdown sensitizes cancer cells to gemcitabine. To determine whether STRN4 suppression can sensitize cancer cells to anticancer drugs, we tested gemcitabine, a nucleoside analog used for pancreatic cancer treatment, in KP4 pancreatic cancer cells. To avoid the toxicity of the transfection reagent, we established KP4 cells that constitutively expressed two different shRNA targeting STRN4 (shSTRN4-1 and shSTRN4-2) as well as control shRNA-expressing cells (shCtrl). The expression of STRN4 was reduced in both the shSTRN4-1 and shSTRN4-2 cells (Fig. 4a). These cells were cultured in the presence of various concentrations of gemcitabine, and cell growth was assessed. As shown in Figure 4(b), the STRN4-depleted KP4 cells were more sensitive to gemcitabine treatment than the control KP4 cells. To further confirm the increased sensitivity to gemcitabine, we performed a TUNEL assay. shCtrl and shSTRN4-1 cells were incubated with or without gemcitabine for 72 h and then analyzed. We observed a significant increase in apoptotic cells depleted of STRN4 (Fig. 4c). These results indicate that knockdown of STRN4 can sensitize cells to gemcitabine treatment.

STRN4 knockdown suppresses cancer cell growth and metastasis in mice. We next investigated the growth of STRN4 knockdown cells in mice using shRNA-expressing KP4 cells. shCtrl and shSTRN4-1 KP4 cells were injected s.c. into the femoral area of nude mice, and tumor formation was examined. Both cell lines formed five subcutaneous tumors out of a total of five injected sites. The tumor formation of the shSTRN4-1 cells was suppressed compared with the tumor formation of the shCtrl cells (Fig. 5a). The mice were killed 5 weeks after tumor cell injection, and the tumor weight was then determined. The average weight of the shSTRN4-1 cell-derived tumors was significantly reduced compared with that of the shCtrl cells (Fig. 5b). We also examined the effect of STRN4

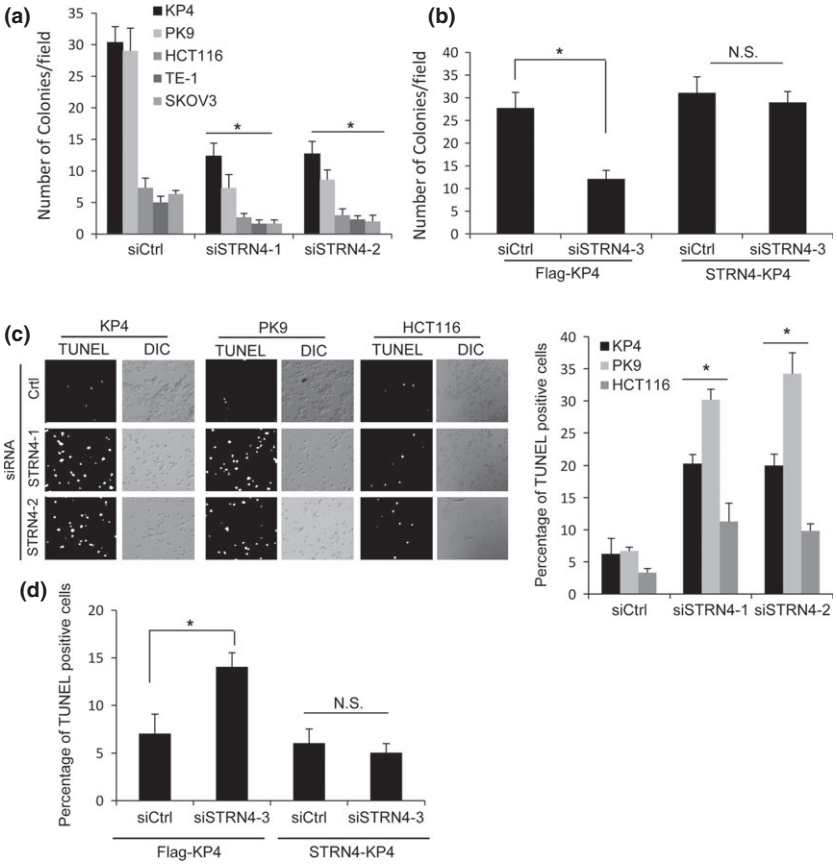

Fig. 3. STRN4 depletion induces anoikis. (a) Cells were transfected with siRNA and subjected to the soft agar colony formation assay. The graph indicates the average number of colonies per field. Three independent experiments were performed, and the data are shown as the mean ± SD (*$P < 0.05$, compared with Ctrl siRNA-transfected cells). (b) Flag-KP4 and STRN4-KP4 cells were transfected with siRNA and then subjected to the soft agar colony formation assay. The graph indicates the average number of colonies per field. Three independent experiments were performed, and the data are shown as the mean ± SD (*$P < 0.05$; NS, not significant). (c) siRNA-transfected cells were cultured in suspension for 24 h and then subjected to TUNEL assay. Representative images of TUNEL assay results are shown. The graph shows the percentage of apoptotic cells from three independent experiments. The data are shown as the mean ± SD (*$P < 0.05$, compared with Ctrl siRNA-transfected cells). (d) Flag-KP4 and STNR4-KP4 cells were subjected to anoikis assay. The graph shows the percentage of apoptotic cells from three independent experiments. The data are shown as the mean ± SD (*$P < 0.05$, NS, not significant).

depletion on the metastasis of KP4 cells. Both shCtrl and shSTRN4-1 cells were injected in the lateral tail vein of mice, and metastasis in the lung and liver was examined. Three out of the five mice injected with shCtrl cells formed metastatic foci in the lung or liver; however, we did not observe any metastatic foci in the lung and liver of the mice injected with shSTRN4-1 (Fig. 5c). We maintained the mice for 8 weeks after tumor injection. Three shCtrl-injected mice died within 8 weeks, but all the mice injected with shSTRN4-1 cells survived for over 8 weeks (Fig. 5d). These results suggest that STRN4 is associated with tumor formation and metastasis.

Discussion

In this report, we show that STRN4 is expressed in multiple cancer cell lines and that depletion of STRN4 in some cancer

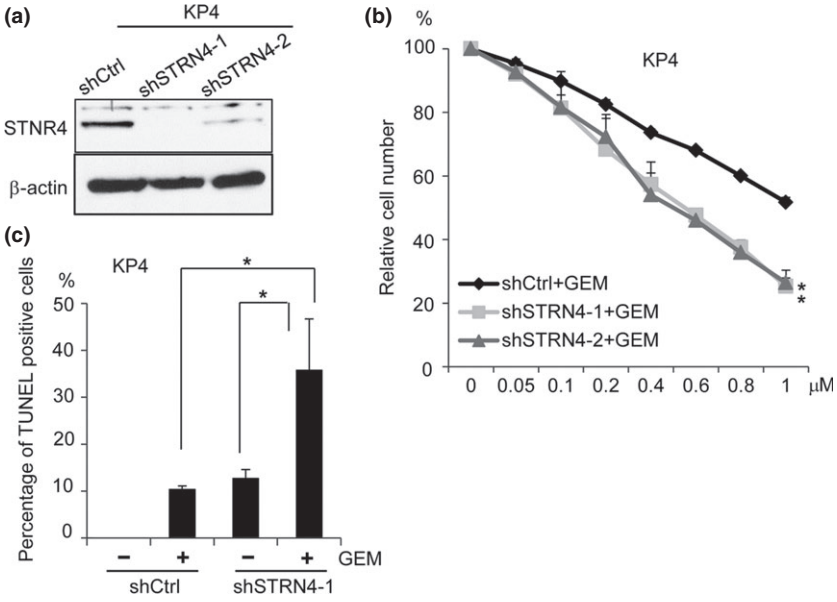

Fig. 4. Depletion of STRN4 sensitizes KP4 cells to gemcitabine. (a) Expression of STRN4 was examined via immunoblot. (b) The cells were cultured in the presence of various concentrations of gemcitabine, and the proliferation ratio was evaluated. Data are presented as percent growth of cells treated without gemcitabine. (c) The cells were cultured in the presence of 1 μM of gemcitabine for 72 h and then subjected to TUNEL assay. The graph shows the percentage of apoptotic cells from three independent experiments. The data are shown as the mean ± SD (*$P < 0.05$).

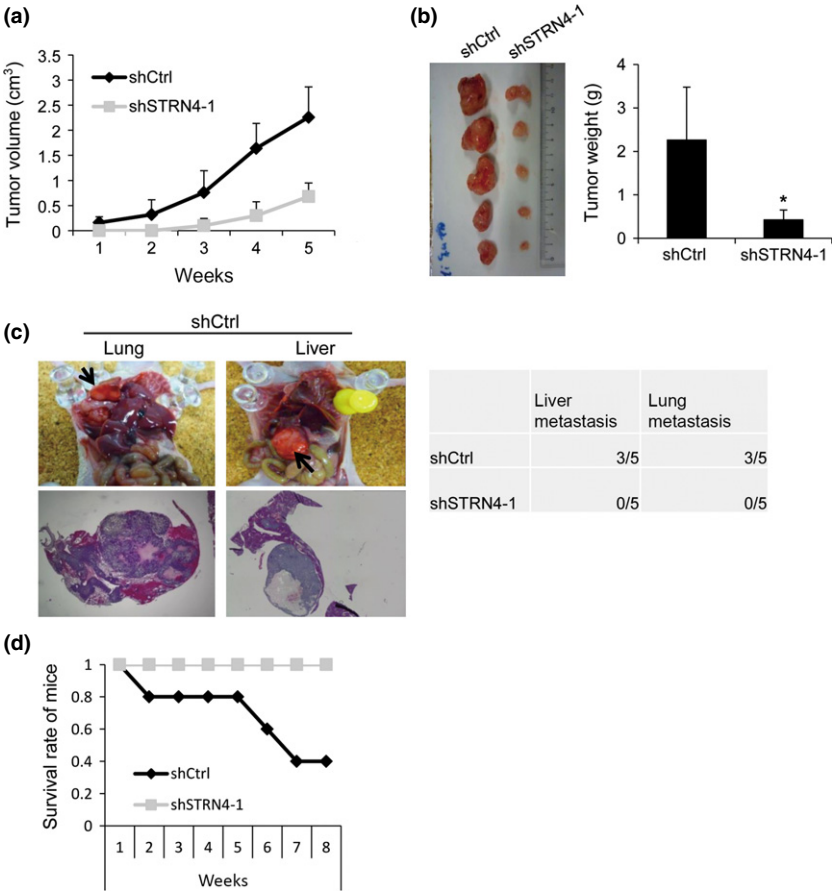

	Liver metastasis	Lung metastasis
shCtrl	3/5	3/5
shSTRN4-1	0/5	0/5

Fig. 5. Depletion of STRN4 suppresses tumor proliferation and metastasis in mice. (a) shCtrl and shSTRN4-1 KP4 cells were injected s.c. into the femurs of mice, and the tumor volume was then measured. The graph shows the average volume of five tumors corresponding to each cell line. (b) Five weeks after tumor injection, the mice were killed and the tumor weight was measured. The picture shows the extracted tumors, and the graph indicates the average tumor weight of the five tumors derived from each cell line (*$P < 0.05$). (c) Cells were injected into the lateral tail vein of mice, and metastasis in the lung and liver was examined. Representative images of lung and liver with tumor metastasis are shown. The images in the lower panel are HE-stained tumor foci in the lung and liver. (d) Survival curve of mice injected i.v. with shCtrl or shSTRN4-1 KP4 cells. The surviving mice were killed 8 weeks after injection.

cell lines inhibits cell cycle progression and induces apoptosis. Depletion of STRN4 reduced migration, invasion and survival in suspension conditions. In addition, STRN4 knockdown increased the sensitivity of KP4 cells to gemcitabine. Striatins have been shown to associate with multiple protein kinases that play a role in tumor progression. Connector of kinase to AP-1 (CKA) is a homolog of striatin family proteins in *Drosophila melanogaster*. CKA promotes AP-1 activation and associates with HEP and BSK, which are human homologs of JNKK (Jun kinase kinase) and JNK (Jun kinase), respectively.[27] AP-1, which is a heterodimeric transcription factor comprising c-Fos, c-Jun, ATF and JDP family proteins, plays a pivotal role in the progression of numerous tumor types. We have previously reported that STRN4 directly associates with MINK1, TNIK and MAP4K4.[13] MINK1 is activated by Ras activation and mediates p38 activation during growth arrest and senescence.[24] Both TNIK and MAP4K4 exert tumor-promoting activity. TNIK phosphorylates T-cell factor 4 (TCF4) to activate Wnt signaling and stimulate colorectal cancer cell proliferation.[26] MAP4K4 is overexpressed in many types of human cancer, and silencing of MAP4K4 inhibits tumor cell migration and proliferation.[25,28] STRN4 has been reported to regulate the activity of associating kinases;[13] thus, depletion of STRN4 may affect the activity of these kinases and suppress signaling pathways critical for the invasion and survival of cancer cells.

Recently, proteomic analysis has revealed that striatin family members are core components of a large multiprotein complex known as STRIPAK. The STRIPAK complex contains catalytic and structural subunits of PP2A, striatins, Mob3, STRIP1/2, and other weakly associating proteins such as CCM3/PDCD10, members of germinal center kinases, CTTNBP2NL and SLMAP. The STRIPAK and STRIPAK-like complex are found in a wide range of species ranging from fungi to humans.[23] In *Drosophila melanogaster*, the STRIPAK complex associates with Hpo (MST1/2 in mammals), a protein kinase involved in cell proliferation, and inactivates the Hpo-dependent signaling pathway.[29] The STRIPAK complex is required for mitosis and cytokinesis of *Schizosaccharomyces pombe*,[21] as well as growth and sexual development in filamentous fungi.[23] In mammals, the exact physiological function of STRIPAK remains to be determined, but proteomic analysis has revealed that some STRIPAK components, including striatins, STRIP1/2 and CTTNBP2NL, associate with dynein, a motor protein involved in cell division and intracellular transport.[30] These studies have shown that the STRIPAK complex plays a crucial role in a diverse set of fundamental cellular functions. As STRN4 is a core component of STRIPAK, depletion of STRN4 may disrupt organization of the STRIPAK complex and suppress invasion and survival of cells. CCM3/PDCD10 has been reported to regulate the activity of protein kinases, such as MST3 and MST4.[31–33] MST4 is known to promote cellular transformation by modulating the activity of the ERK pathway. Therefore, STRN4 depletion may disrupt signaling pathways mediated by CCM3/PDCD and its associated kinases.[34,35] Although further analysis is needed, the STRIPAK complex may represent an interesting target for the development of novel cancer therapeutics.

Acknowledgments

We would like to thank the members of the Division of Cancer Biology for helpful discussions and technical assistance. This research was partially funded by a grant from the Naito Foundation and the Ministry of Education, Culture, Sports, Science and Technology of Japan.

Disclosure Statement

The authors have no conflict of interest to declare.

References

1 Castets F, Bartoli M, Barnier JV *et al.* A novel calmodulin-binding protein, belonging to the WD-repeat family, is localized in dendrites of a subset of CNS neurons. *J Cell Biol* 1996; **134**: 1051–62.
2 Muro Y, Chan EK, Landberg G, Tan EM. A cell-cycle nuclear autoantigen containing WD-40 motifs expressed mainly in S and G2 phase cells. *Biochem Biophys Res Commun* 1995; **207**: 1029–37.
3 Castets F, Rakitina T, Gaillard S, Moqrich A, Mattei MG, Monneron A. Zinedin, SG2NA, and striatin are calmodulin-binding, WD repeat proteins principally expressed in the brain. *J Biol Chem* 2000; **275**: 19970–7.
4 Bartoli M, Monneron A, Ladant D. Interaction of calmodulin with striatin, a WD-repeat protein present in neuronal dendritic spines. *J Biol Chem* 1998; **273**: 22248–53.
5 Gaillard S, Bartoli M, Castets F, Monneron A. Striatin, a calmodulin-dependent scaffolding protein, directly binds caveolin-1. *FEBS Lett* 2001; **508**: 49–52.
6 Gaillard S, Bailly Y, Benoist M *et al.* Targeting of proteins of the striatin family to dendritic spines: role of the coiled-coil domain. *Traffic* 2006; **7**: 74–84.
7 Kachidian P, Vuillet J, Bartoli M, Castets F, Nieoullon A, Kerkerian-Le Goff L. Relationships between striatin-containing neurons and cortical or thalamic afferent fibres in the rat striatum. An ultrastructural study by dual labelling. *Neuroscience* 1998; **85**: 111–22.
8 Salin P, Kachidian P, Bartoli M, Castets F. Distribution of striatin, a newly identified calmodulin-binding protein in the rat brain: an in situ hybridization and immunocytochemical study. *J Comp Neurol* 1998; **397**: 41–59.
9 Bartoli M, Ternaux JP, Forni C *et al.* Down-regulation of striatin, a neuronal calmodulin-binding protein, impairs rat locomotor activity. *J Neurobiol* 1999; **40**: 234–43.
10 Lu Q, Pallas DC, Surks HK, Baur WE, Mendelsohn ME, Karas RH. Striatin assembles a membrane signaling complex necessary for rapid, nongenomic activation of endothelial NO synthase by estrogen receptor alpha. *Proc Natl Acad Sci U S A* 2004; **101**: 17126–31.
11 Breitman M, Zilberberg A, Caspi M, Rosin-Arbesfeld R. The armadillo repeat domain of the APC tumor suppressor protein interacts with Striatin family members. *Biochim Biophys Acta* 2008; **1783**: 1792–802.
12 Moreno CS, Park S, Nelson K *et al.* WD40 repeat proteins striatin and S/G (2) nuclear autoantigen are members of a novel family of calmodulin-binding proteins that associate with protein phosphatase 2A. *J Biol Chem* 2000; **275**: 5257–63.
13 Hyodo T, Ito S, Hasegawa H *et al.* Misshapen-like kinase 1 (MINK1) is a novel component ofstriatin-interacting phosphatase and kinase (STRIPAK) and is required for the completion of cytokinesis. *J Biol Chem* 2012; **287**: 25019–29.
14 Benoist M, Gaillard S, Castets F. The striatin family: a new signaling platform in dendritic spines. *J Physiol Paris* 2006; **99**: 146–53.
15 Gordon J, Hwang J, Carrier KJ *et al.* Protein phosphatase 2a (PP2A) binds within the oligomerization domain of striatin and regulates the phosphorylation and activation of the mammalian Ste20-Like kinase Mst3. *BMC Biochem* 2011; **12**: 54.
16 Janssens V, Goris J. Protein phosphatase 2A: a highly regulated family of serine/threonine phosphatases implicated in cell growth and signalling. *Biochem J* 2001; **353**: 417–39.
17 Van Hoof C, Goris J. Phosphatases in apoptosis: to be or not to be, PP2A is in the heart of the question. *Biochim Biophys Acta* 2003; **21640**: 97–104.
18 Goudreault M, D'Ambrosio LM, Kean MJ *et al.* A PP2A phosphatase high density interaction network identifies a novel striatin-interacting phosphatase and kinase complex linked to the cerebral cavernous malformation 3 (CCM3) protein. *Mol Cell Proteomics* 2009; **8**: 157–71.
19 Kean MJ, Ceccarelli DF, Goudreault M *et al.* Structure-function analysis of core STRIPAK Proteins: a signaling complex implicated in Golgi polarization. *J Biol Chem* 2011; **286**: 25065–75.
20 Bloemendal S, Bernhards Y, Bartho K *et al.* A homologue of the human STRIPAK complex controls sexual development in fungi. *Mol Microbiol* 2012; **84**: 310–23.
21 Frost A, Elgort MG, Brandman O *et al.* Functional repurposing revealed by comparing *S. pombe* and *S. cerevisiae* genetic interactions. *Cell* 2012; **149**: 1339–52.
22 Pracheil T, Liu Z. Tiered assembly of the yeast Far3-7-8-9-10-11 complex at the endoplasmic reticulum. *J Biol Chem* 2013; **288**: 16986–97.
23 Hwang J, Pallas DC. STRIPAK complexes: structure, biological function, and involvement in human diseases. *Int J Biochem Cell Biol* 2014; **47**: 118–48.
24 Nicke B, Bastien J, Khanna SJ *et al.* Involvement of MINK, a Ste20 family kinase, in Ras oncogene-induced growth arrest in human ovarian surface epithelial cells. *Mol Cell* 2005; **20**: 673–85.
25 Collins CS, Hong J, Sapinoso L *et al.* A small interfering RNA screen for modulators of tumor cell motility identifies MAP4K4 as a promigratory kinase. *Proc Natl Acad Sci U S A* 2006; **103**: 3775–80.
26 Shitashige M, Satow R, Jigami T *et al.* Traf2- and Nck-interacting kinase is essential for Wnt signaling and colorectal cancer growth. *Cancer Res* 2010; **70**: 5024–33.
27 Chen HW, Marinissen MJ, Oh SW *et al.* CKA, a novel multidomain protein, regulates the JUN N-terminal kinase signal transduction pathway in Drosophila. *Mol Cell Biol* 2002; **22**: 1792–803.
28 Liu AW, Cai J, Zhao XL *et al.* ShRNA-targeted MAP4K4 inhibits hepatocellular carcinomagrowth. *Clin Cancer Res* 2011; **17**: 710–20.
29 Couzens AL, Knight JD, Kean MJ *et al.* Protein interaction network of the mammalian Hippo pathway reveals mechanisms of kinase-phosphatase interactions. *Sci Signal* 2013; **6**: rs15.
30 Hutchins JR, Toyoda Y, Hegemann B *et al.* Systematic analysis of human protein complexes identifies chromosome segregation proteins. *Science* 2010; **328**: 593–9.
31 Fidalgo M, Fraile M, Pires A, Force T, Pombo C, Zalvide J. CCM3 /PDCD10 stabilizes GCKIII proteins to promote Golgi assembly and cell orientation. *J Cell Sci* 2010; **123**: 1274–84.
32 Fidalgo M, Guerrero A, Fraile M, Iglesias C, Pombo CM, Zalvide J. Adaptor protein cerebral cavernous malformation 3 (CCM3) mediates phosphorylation of the cytoskeletal proteins ezrin/radixin/moesin by mammalian Ste20-4 to protect cells from oxidative stress. *J Biol Chem* 2012; **287**: 11556–65.
33 Ma X, Zhao H, Shan J *et al.* PDCD10 interacts with Ste20-related kinase MST4 to promote cell growth and transformation via modulation of the ERK pathway. *Mol Biol Cell* 2007; **18**: 1965–78.
34 Lin JL, Chen HC, Fang HI, Robinson D, Kung HJ, Shih HM. MST4, a new Ste20-related kinase that mediates cell growth and transformation via modulating ERK pathway. *Oncogene* 2001; **20**: 6559–69.
35 Lin ZH, Wang L, Zhang JB *et al.* MST4 promotes hepatocellular carcinoma epithelial-mesenchymal transition and metastasis via activation of the p-ERK pathway. *Int J Oncol* 2014; **45**: 629–40.

Supporting Information

Additional supporting information may be found in the online version of this article:

Fig. S1. Depletion of STRN4 induces apoptosis.

Fig. S2. Depletion of STRN4 suppresses migration and invasion.